

PHOTOCHEMISTRY

Imaging the short-lived hydroxyl-hydronium pair in ionized liquid water

M.-F. Lin^{1*}, N. Singh², S. Liang³, M. Mo¹, J. P. F. Nunes⁴, K. Ledbetter^{5,6}, J. Yang^{1,5†}, M. Kozina¹, S. Weathersby¹, X. Shen¹, A. A. Cordones⁵, T. J. A. Wolf^{1,5}, C. D. Pemmaraju⁷, M. Ihme^{2*}, X. J. Wang^{1*}

The radiolysis of water is ubiquitous in nature and plays a critical role in numerous biochemical and technological applications. Although the elementary reaction pathways for ionized water have been studied, the short-lived intermediate complex and structural dynamic response after the proton transfer reaction remain poorly understood. Using a liquid-phase ultrafast electron diffraction technique to measure the intermolecular oxygen...oxygen and oxygen...hydrogen bonds, we captured the short-lived radical-cation complex OH(H₃O⁺) that was formed within 140 femtoseconds through a direct oxygen...oxygen bond contraction and proton transfer, followed by the radical-cation pair dissociation and the subsequent structural relaxation of water within 250 femtoseconds. These measurements provide direct evidence of capturing this metastable radical-cation complex before separation, thereby improving our fundamental understanding of elementary reaction dynamics in ionized liquid water.

The radiolysis of liquid water is of fundamental importance to a wide range of biomedical, chemical, and engineering processes (1, 2), including radiotherapy (3, 4), surgical precision optimization (4), water disinfection (5), and corrosion damage in nuclear waste storage and reactors (6). The ionization of liquid water leads to the formation of hydrated electrons and water cations (H₂O⁺) that undergo ultrafast proton transfer to produce hydroxyl radicals (OH) and hydronium cations (H₃O⁺) within <100 fs (7, 8). At the same time, the ionized electron in the excited *p*-like state is either rapidly solvated by neighboring water molecules in ~50 fs or is followed by the nonadiabatic relaxation of the *p*-like state to the *s*-like state in ~50 fs and the solvent structure relaxation on the ground-electronic *s*-like state within a picosecond (9–11). The hydrated and thermalized electrons recombine with the ion cores and hydroxyl radicals through geminate and non-geminate recombinations that evolve on time scales between tens of picoseconds and nanoseconds (12, 13). Previous time-resolved measurements reported lifetimes of transient species and corresponding changes of local electronic structures for the first coordinated shell in ionized liquid water (7, 8, 12–19). However, direct measurements of the extended molec-

ular structure in the proton-transfer reaction coordinates leading to the formation of the radical-cation pair, and the following dissociation and nonradiative structural relaxation, have not been reported because of limitations of time-resolved approaches. In particular, capturing the change in the bond distance of an ultrafast chemical reaction requires diffraction methods with large momentum transfer and femtosecond temporal resolution. Such capabilities are provided by our electron diffraction technique, which directly probes the Coulomb potential of the molecules, thereby enabling simultaneous measurements of the O...H and O...O intermolecular bonds. This method is different from x-ray diffraction, which is specifically sensitive to the O...O bond distance in liquid water (20). Probing this intermolecular O...H network is critical for understanding the fundamental reaction mechanisms involving the hydrogen-bond interaction in ionized water. Here, we report femtosecond electron diffraction measurements of the intermolecular O...H and O...O bond structures within OH(H₃O⁺) radical-cation pairs. These time-resolved measurements revealed the presence and structure of the solvated OH(H₃O⁺) radical-cation pair that was formed at ~140 fs, directly confirming previous theoretical results (8, 21–26) suggesting that hydronium cations and hydroxyl radicals dominate the initial structural dynamic response in the laser ionization of water.

The recent development of the liquid-phase mega-electron volt ultrafast electron diffraction (MeV-UED) instrument (27, 28) made it feasible to measure the structural dynamics of ionized liquid water in real time. Figure 1A shows the schematic of the relativistic femtosecond MeV-UED system. A focused 800 nm laser with ~65 ± 5 fs pulse width was used to ionize a liquid water sheet of ~100 nm thickness through multiphoton absorption. The

ionization by the high-energy laser pulse-generated H₂O⁺ and the subsequent chemical reactions in the ionized water were probed by the electron beam (violet). The measured diffraction signal in momentum space between 0.5 and 11.5 Å⁻¹ was converted to the atomic pair distribution function in real space to directly examine the molecular structural dynamics of the ionized liquid water. The azimuthally integrated electron diffraction pattern is shown by the blue curve in Fig. 1B. The scattering signal contained both inelastic and elastic components, which are separated using a power fit method at a low *Q* range (37). The magenta dashed line is the background signal containing the inelastic scattering and the atomic elastic scattering. The difference between the curves is shown by the red-shaded area, which represents the information of the elastic molecular scattering of the liquid water. This elastic scattering qualitatively agreed with our molecular dynamics (MD) simulations using an independent atom model that incorporated the scattering intensity calculation using the TIP4P/2005 force field for the structure of liquid water at 290 K (cyan line) (29). Details of MD simulations are provided in the supplementary materials. Figure 1C displays the charge-pair distribution function (CPDF) of the liquid water obtained from transforming the azimuthally integrated electron diffraction signal in Fig. 1B (30). The CPDF contains all electron-electron, electron-nucleus, and nucleus-nucleus pairs. The corresponding signs and intensities are determined by the product of the two charge particles. The CPDF allowed us to inspect the liquid water structure in physical space. Figure 1C shows four distinct peaks located at 1.8, 2.9, 4.6, and 6.9 Å, which corresponded to the intermolecular O...H bond associated with the hydrogen-bond network and the O...O bond distances in the first, second, and third shell of the neutral water, respectively. The intramolecular O–H bond at ~1 Å, however, could not be determined because of the obscuration of intra-atomic elastic scattering (30). Note that the H...*e*_{aq}⁻ and H...H signal were too weak to be detected by the electron diffraction because of its low scattering cross section (i.e., H...*e*_{aq}⁻ and H...H are ~0.001% and ~4% compared with O...O, respectively). In this work, we examined the O...O and O...H intermolecular coordination layers of ionized water.

Figure 2A illustrates the key mechanisms of the laser ionization of liquid water. The instantaneously formed H₂O⁺ cation, generated through the nonlinear electronic excitation of the ¹b₁ valence band of water (7), reacted first with a neighboring water molecule to produce a transient OH(H₃O⁺) pair, followed by the dissociation into an individual OH radical and an H₃O⁺ cation. The ionized electron was solvated by the surrounding water molecules

¹SLAC National Accelerator Laboratory, Menlo Park, CA 94025, USA. ²Department of Mechanical Engineering, Stanford University, Stanford, CA 94305, USA. ³Department of Chemistry, Stanford University, Stanford, CA 94305, USA. ⁴Department of Physics and Astronomy, University of Nebraska–Lincoln, Lincoln, NE 68588, USA. ⁵Stanford PULSE Institute, SLAC National Accelerator Laboratory, Menlo Park, CA 94025, USA. ⁶Department of Physics, Stanford University, Stanford, CA 94305, USA. ⁷SIMES, SLAC National Accelerator Laboratory, Menlo Park, CA 94025, USA. *Corresponding author. Email: mfucb@slac.stanford.edu (M.-F.L.); mihme@stanford.edu (M.I.); wangxj@slac.stanford.edu (X.J.W.)

†Present address: Department of Chemistry, Tsinghua University, Beijing, China.

within the first 200 fs. Furthermore, the multiphoton ionization of the liquid water resulted in thermal heating within subpicosecond time scales (15, 19, 31, 32), which is illustrated by the first-order rate constant, k . This signal resembling thermal heating was reported in several studies using the optical absorption spectral shift of solvated electrons in laser-heated water and the laser-induced structural change using x-ray diffraction as a probe (31, 32). Using MeV-UED, we directly captured the structural-dynamic changes of the radicals and cations associated with the proton-transfer coordinates and measured the effects of the laser heating of water from the nonradiative relaxation process.

Figure 2B displays the measured differential pair distribution function, $\Delta PDF(r, t)$, of the ionized liquid water. A detailed analysis of the data is provided in the supplementary materials. Negative values of ΔPDF , shown in blue, indicated a decrease of the pair density for the coordination-shell distances of neutral water at 1.8, 2.8, 4.5, and 7 Å caused by structural changes during the laser ionization. The depletion at 1.8 Å corresponded to the disruption of the intermolecular O...H bond associated with the hydrogen-bond network of liquid water. The disappearance of the signal at 2.8, 4.5, and 7 Å corresponded to the change of the first, second, and third O...O coordination shells, respectively. By contrast, the appearance of shorter new atomic-pair distances, shown in red, was associated with O...H and O...O intermolecular bonds. These results showed a clear onset of the changes in the pair distance at time $t = 0$, marked by the black dashed line. A fast decay component of several hundred femtoseconds was observed at 1.4 and 2.4 Å, and the difference signals at distances larger than 3 Å evolved with a similar time constant. Beyond ~500 fs, the ΔPDF revealed similar features with minor variations in relative amplitude toward longer delay times. These results indicated that there was a minimum of two components that represented short- and long-lived structural-dynamic processes.

To analyze these data as a function of bond distance and delay time, we applied a global fit using singular value decomposition and a first-order kinetic model to deconvolve the transient components and kinetics (analysis is shown in figs. S2 to S4). The fit yielded an instrument response function (IRF) of 140 ± 6 fs in full width at half maximum (FWHM), which was sufficient to capture the transient OH (H_3O^+) radical-cation pair in water. The obtained first-order time constant from the kinetic model is 252 ± 7 fs. We ascribed this time constant to an ultrafast OH(H_3O^+) pair dissociation in concomitance with the relaxation of the water structure that resembled the heating process of the ionized liquid water (21). This ultrafast structural response in ionized water was pos-

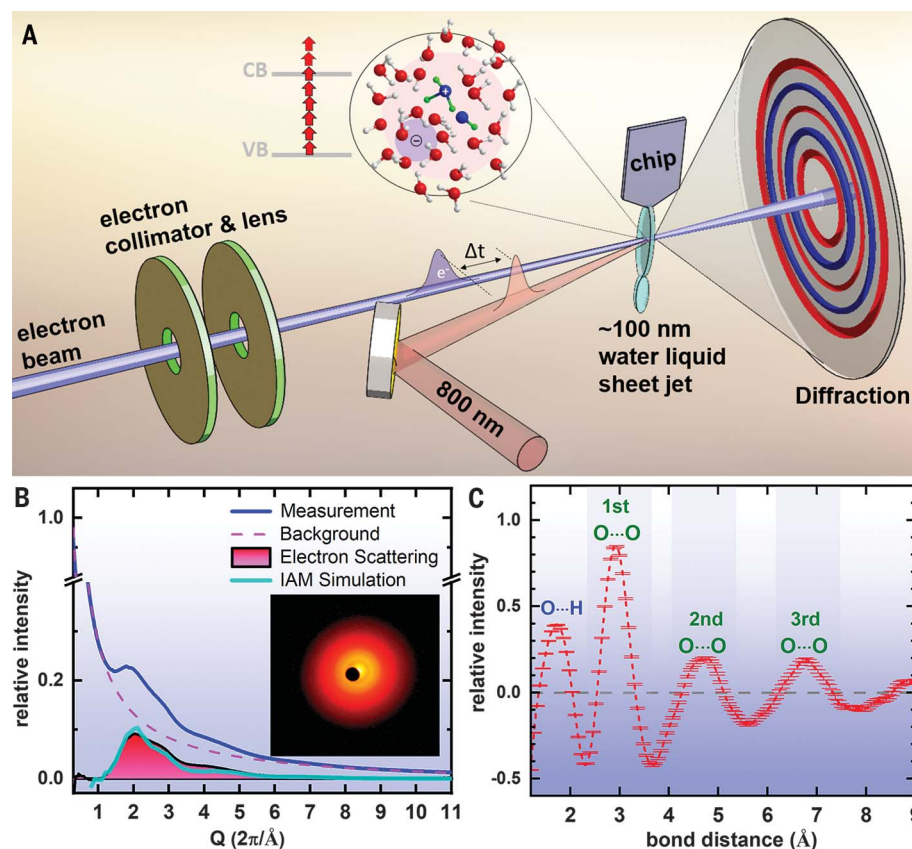


Fig. 1. Ultrafast electron diffraction measurement of ionized liquid water. (A) Schematic of the MeV-UED system used to capture reactive transient structures in ionized liquid water. The electron bunch is accelerated and compressed to 3.7 MeV and ~90 fs, respectively, for the measurement of a thin liquid water sheet jet of ~100 nm thickness. A two-dimensional detector was placed ~3.1 m downstream of the interaction point to collect the scattered electrons. A pump-laser beam at 800 nm excited the valence band (VB) electron in water nonlinearly to the conduction band (CB) and initiates the chemical reactions. The reaction dynamics were interrogated by a delayed mega-electron volt electron beam. (B) Azimuthally integrated electron-diffraction pattern obtained from a thin liquid-sheet water jet at 291 ± 1 K (blue). The smooth background and the elastic scattering of the MeV-UED through the liquid water sheet are shown by the dashed magenta curve and red-shaded area, respectively. Simulation results from the independent atom model are shown by the cyan curve. The raw electron diffraction pattern is shown in the inset with its intensity in logarithmic scale. The center of the diffraction pattern is intentionally offset on the detector hole to collect the low momentum scattering signal. (C) CPDF of the liquid water calculated from the measured electron diffraction signal in (B). CPDF displays several distinct peaks located at 1.8, 2.9, 4.6, and 6.9 Å, corresponding to intermolecular O...H, first shell O...O, second shell O...O, and third shell O...O bonds, respectively. The intermolecular O...H bond at 1.8 Å represents the hydrogen bond, which plays an important role in the structural dynamics of the reactive species in ionized liquid water. The error bars represent the 68% confidence interval from repeated experimental measurements (i.e., SD).

tulated from time-resolved x-ray diffraction studies (31).

Figure 2C shows the transient structure of ionized water at the delay time averaged between 0 and 200 fs. The newly formed peaks in ΔPDF at 1.4 and 2.4 Å corresponded to the measured O...H and O...O bond distances of the solvated OH(H_3O^+) pair before separation. These results agreed well with predictions from ab initio MD simulations, suggesting similar intermolecular bond distances (green symbols in Fig. 2E) (8, 21–26). These measurements provided direct experimental evidence of the transient structure of the OH(H_3O^+)

radical-cation pair in ionized liquid water before its separation. The contracted intermolecular O...H and O...O bonds after the proton transfer from the $\text{H}_2\text{O}(\text{H}_3\text{O}^+)$ reaction center were directly imaged by our electron diffraction measurements. The structural features at 1.4 and 2.4 Å from the global fit were also short-lived and disappeared within 252 ± 7 fs (blue curves in Fig. 2F). These fast structural-dynamic changes indicated that the separation of the OH(H_3O^+) pair within this short time window occurred because of the subsequent proton propagation from H_3O^+ to the outer shell neutral water within ~250 fs and

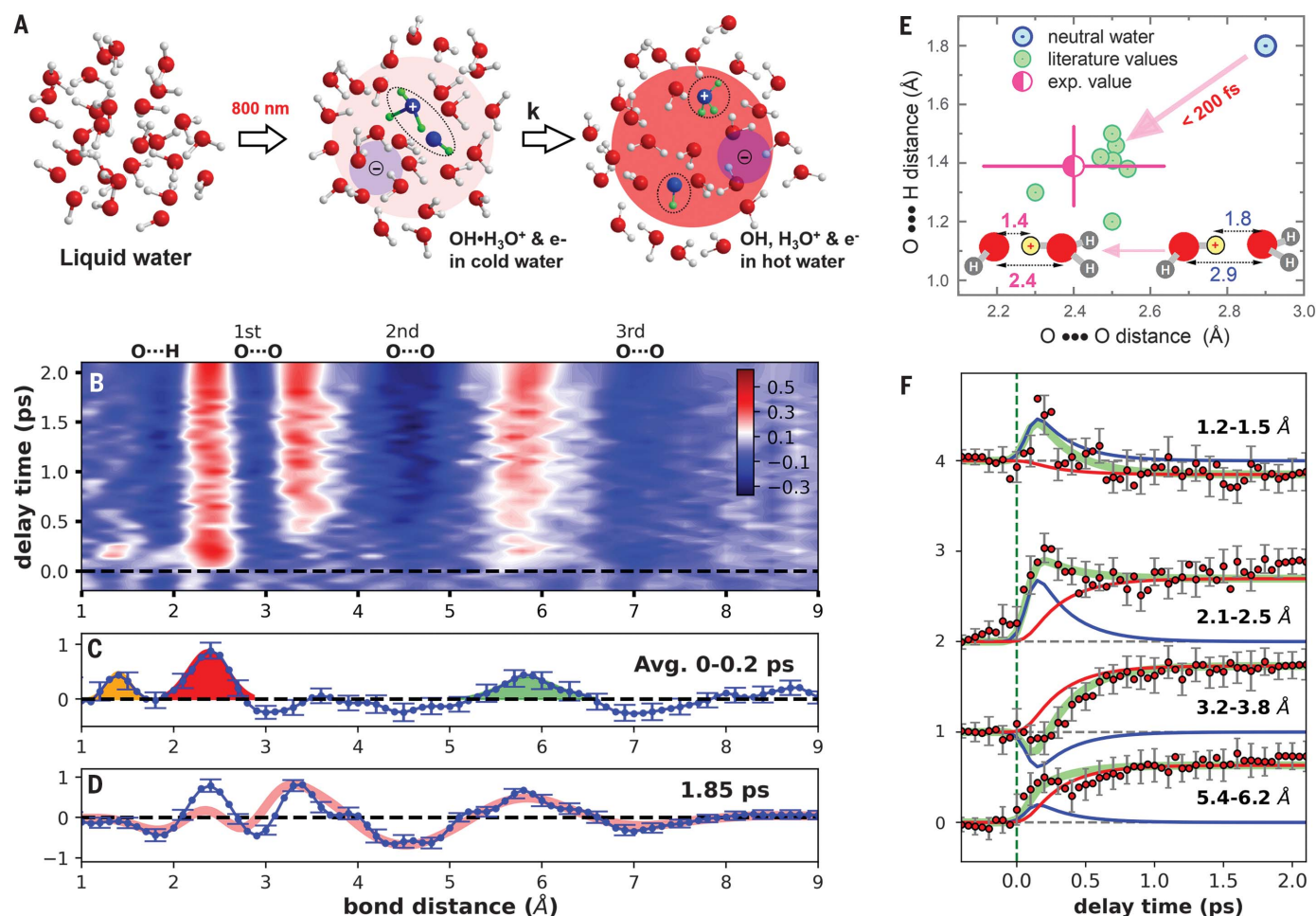


Fig. 2. Time-resolved electron diffraction of OH...H₃O⁺ pair and nonradiative decay. (A) Ionization of liquid water and formation of solvated hydronium, hydroxyl radical, and electron, followed by the local thermalization through nonradiative relaxation. (B) Transient $\Delta PDF(r,t)$ of the ionized liquid water. Red and blue areas represent the ionization-induced pair-density formation and depletion of the liquid water, respectively. The horizontal black dashed line marks the time-zero location of the signal. (C and D) Selected experimental transient diffraction signals at averaged delay from 0 to 0.2 ps (C) and at 1.85 ps (D), respectively, from (B). Error bars correspond to a 68% confidence interval from the SD from repeated experimental measurements. The orange, red, and green areas in (C) indicate the formation of new intermolecular O...H and O...O bonds in the OH(H₃O⁺) pair and the thermal

heating, respectively. (E) Proton transfer reaction coordinates during the first 200 fs. Comparison of the intermolecular O...H and O...O bond distances in liquid water and hydroxyl/hydronium pair from experimental (pink) and literature values (green). The vertical and horizontal bars on the experimental data represent the FWHM distribution of the corresponding signal peaks in (C). (F) Time-resolved bond distance changes at integrated areas of 1.35 ± 0.15 , 2.3 ± 0.2 , 3.5 ± 0.3 , and 5.8 ± 0.4 Å. Green solid curves and red-filled circles are the global fitted and experimental results, respectively. The blue and red curves denote the fast and slow components from the global fit for each selected bond range. The vertical green dashed line marks time zero. The error bars are shown with the SD, which represents the 68% confidence interval from repeated experimental measurements.

agreed with predictions (8, 21, 23). After the radical-cation pair dissociation, the new O...O bond distance between H₃O⁺ and H₂O appeared near ~ 2.4 to 2.5 Å (17). This feature also coincided with the later generation of hot water associated with the O...H network (see fig. S6). These two processes contributed to the growth of the signal at 2.4 Å at a longer delay time. Beyond the first water layer, we also observed a signal of lower intensity at bond distances centered at 3.4 and 5.8 Å at ~ 100 fs. This structural change appeared to evolve more slowly than the OH(H₃O⁺) pair formation at ~ 140 fs (bottom panel in Fig. 2F). We attributed these structural features, together with the component at 2.4 Å beyond

~ 500 fs, to the laser heating and the re-orientation of the surrounding liquid water in response to the ionization center (21).

In addition to the ultrafast formation of OH(H₃O⁺) pairs at ~ 140 fs (IRF), we observed a slower component with a time constant of 252 ± 7 fs (Fig. 2D). The corresponding kinetics are shown by the red curves in Fig. 2F. The separation of the OH(H₃O⁺) pair through the following proton transfer to neighboring water and the structural change in response to the excitation center occurred at similar time scales and explained our time constant of 252 ± 7 fs (21, 23). Note that this time scale was far shorter than the longitudinal thermal expansion of water at ~ 67 ps by laser excita-

tion. This process could be associated with a temperature jump that contributed to the change in the diffraction signal at constant density (33). The transient signal of the structural relaxation resembled the heating of the neutral water system and could be described by hot water in the dilute limit of transient species (see section 3b in the supplementary materials). To quantify this energy deposition and temperature rise in ionized liquid water, we performed time-dependent density functional theory simulations to estimate the photon energy that was deposited in water by an 800-nm laser pulse with a peak intensity of $2 \pm 1 \times 10^{13}$ W/cm² (see section 3c in the supplementary materials). These simulations

showed <1% total photoexcitation of the valence band electrons to the conduction band and energy states above the ionization potential of liquid water. The low excitation fraction agreed with other experiments at similar peak intensities (17). The estimated maximum local temperature increase, ΔT , from the deposited photon energy was ~ 320 K (analysis is provided in section 3d in the supplementary materials). Previous studies have examined ultrafast thermal heating through direct laser excitations with infrared and ultraviolet light sources (15, 31). These experiments reported a tens of kelvins temperature rise within a picosecond time scale at laser peak intensities approximately an order of magnitude lower than the current study. Recently, several simulation studies have suggested that it is possible to achieve temperature jumps of hundreds of kelvins within a few hundreds of femtoseconds by terahertz excitations (34). Thus, a fast temperature rise by hundreds of kelvins by laser excitation is feasible. The pink trace in Fig. 2D represents the ΔPDF between hot water at 610 K and water at 290 K from our MD simulations, showing qualitative agreement with our measurements. Thus, our simulations provide a qualitative description of the thermal excitation after the ionization of the liquid water. A detailed microscopic picture of the structural reorientation associated with energy redistribution in response to the ionization center, $\text{OH}(\text{H}_3\text{O}^+)$, requires a full ab initio simulation of liquid water, which is beyond the scope of the current study.

In summary, our MeV-UED measurements revealed two important structural-dynamic processes of laser-ionized liquid water. First, we observed an ultrafast chemical reaction in ionized liquid water that produced short-lived $\text{OH}(\text{H}_3\text{O}^+)$ radical-cation pairs and their rapid dissociation to form separated OH and H_3O^+ radicals at a time constant of 252 ± 7 fs. The formation of the radical-cation pair started from the H-bonded $\text{H}_2\text{O}^+\cdots\text{H}_2\text{O}$ pair, which underwent an O \cdots O intermolecular bond contraction and a proton transfer between two oxygen atoms. This ultrafast chemical reaction exceeded the temporal resolution currently achievable with our MeV-UED instrument. A resolution of ~ 50 fs or higher sensitivity is

necessary to resolve the proton transfer and the contraction of the O \cdots O bond in real time. With improvements proposed for MeV-UED, such as electron pulse compression, high repetition rate, and direct electron detection, we foresee the possibility of capturing proton transfer dynamics in ionized liquid water. Second, the reorientation of the water molecules surrounding the excitation center resulted in a structural change that resembled thermal heating of the liquid water in 252 ± 7 fs. This structural change of the heated water hereafter dominated the following signal in the electron diffraction measurement. Our study not only captured the short-lived and highly reactive radical-cation species but also illustrated the ultrafast structural relaxation near the ionization center that may have a further impact on subsequent chemical reactions in ionized liquid water.

REFERENCES AND NOTES

- B. C. Garrett *et al.*, *Chem. Rev.* **105**, 355–390 (2005).
- J. Ma, F. Wang, M. Mostafavi, *Molecules* **23**, 244 (2018).
- X. Xu, H. Lu, R. Lee, *Front. Bioeng. Biotechnol.* **8**, 488 (2020).
- K. König, I. Riemann, W. Fritzsche, *Opt. Lett.* **26**, 819–821 (2001).
- S. Siahrostami, G. L. Li, V. Viswanathan, J. K. Nørskov, *J. Phys. Chem. Lett.* **8**, 1157–1160 (2017).
- B. Grambow, M. Mostafavi, *Environ. Sci. Process. Impacts* **16**, 2472–2476 (2014).
- Z. H. Loh *et al.*, *Science* **367**, 179–182 (2020).
- O. Marsalek *et al.*, *J. Chem. Phys.* **135**, 224510 (2011).
- Y. Kimura, J. C. Alfano, P. K. Walhout, P. F. Barbara, *J. Phys. Chem.* **98**, 3450–3458 (1994).
- R. M. Young, D. M. Neumark, *Chem. Rev.* **112**, 5553–5577 (2012).
- C. Silva, P. K. Walhout, K. Yokoyama, P. F. Barbara, *Phys. Rev. Lett.* **80**, 1086–1089 (1998).
- S. Kratz, J. Torres-Alacan, J. Urbanek, J. Lindner, P. Vöhringer, *Phys. Chem. Chem. Phys.* **12**, 12169–12176 (2010).
- Y. Muroya *et al.*, *J. Phys. Chem. Lett.* **1**, 331–335 (2010).
- R. A. Crowell, D. M. Bartels, *J. Phys. Chem.* **100**, 17940–17949 (1996).
- R. A. Crowell *et al.*, *J. Phys. Chem. A* **108**, 9105–9114 (2004).
- C. L. Thomsen, D. Madsen, S. R. Keiding, J. Thøgersen, O. Christiansen, *J. Chem. Phys.* **110**, 3453–3462 (1999).
- J. Li, Z. Nie, Y. Y. Zheng, S. Dong, Z. H. Loh, *J. Phys. Chem. Lett.* **4**, 3698–3703 (2013).
- V. Svoboda *et al.*, *Sci. Adv.* **6**, eaaz0385 (2020).
- D. Madsen, C. L. Thomsen, J. Thøgersen, S. R. Keiding, *J. Chem. Phys.* **113**, 1126–1134 (2000).
- K. Amann-Winkel *et al.*, *Chem. Rev.* **116**, 7570–7589 (2016).
- A. Furuhashi, M. Dupuis, K. Hirao, *J. Chem. Phys.* **124**, 164310 (2006).
- P. A. Pieniazek, J. VandeVondele, P. Jungwirth, A. I. Krylov, S. E. Bradforth, *J. Phys. Chem. A* **112**, 6159–6170 (2008).
- H. Tachikawa, *J. Phys. Chem. A* **108**, 7853–7862 (2004).
- R. N. Barnett, U. Landman, *J. Phys. Chem. A* **101**, 164–169 (1997).
- G. H. Gardenier, M. A. Johnson, A. B. McCoy, *J. Phys. Chem. A* **113**, 4772–4779 (2009).
- E. Kamarchik, O. Kostko, J. M. Bowman, M. Ahmed, A. I. Krylov, *J. Chem. Phys.* **132**, 194311 (2010).
- J. D. Koralek *et al.*, *Nat. Commun.* **9**, 1353 (2018).
- J. P. F. Nunes *et al.*, *Struct. Dyn.* **7**, 024301 (2020).
- J. L. F. Abascal, C. Vega, *J. Chem. Phys.* **123**, 234505 (2005).
- J. Yang *et al.*, *Phys. Chem. Chem. Phys.* **23**, 1308–1316 (2021).
- K. Haldrup *et al.*, *J. Phys. Chem. B* **120**, 1158–1168 (2016).
- K. H. Kim *et al.*, *Phys. Rev. Lett.* **125**, 076002 (2020).
- K. S. Kjør *et al.*, *Phys. Chem. Chem. Phys.* **15**, 15003–15016 (2013).
- P. K. Mishra, V. Bettaque, O. Vendrell, R. Santra, R. Welsch, *J. Phys. Chem. A* **122**, 5211–5222 (2018).
- M.-F. Lin, M. Ihme, X. J. Wang, Data for: Imaging the short-lived hydroxyl-hydronium pair in ionized liquid water, *Dryad* (2021); <https://doi.org/10.5061/dryad.9gh3ffhm>.

ACKNOWLEDGMENTS

We thank U. Bergmann from the University of Wisconsin at Madison for discussions on the preparation of this manuscript and B. Schwartz from the University of California at Los Angeles and W. Glover from the New York University at Shanghai, who provided simulation results in support of our search for the signal from the solvated electron in ionized water. **Funding:** The experiment was performed at SLAC MeV-UED and supported in part by the U.S. Department of Energy (DOE) Office of Science, Office of Basic Energy Sciences, SUF Division Accelerator & Detector R&D program, the LCLS Facility, and SLAC under contract Nos. DE-AC02-05CH11231 and DE-AC02-76SF00515. M.M. is supported by the U.S. DOE Office of Science, Laboratory Directed Research and Development program at SLAC under contract DE-AC02-76SF00515 and Fusion Energy Sciences under FWP 100182. N.S. and M.I. are supported by the U.S. DOE Office of Science, Office of Basic Energy Sciences, under award DE-SC0021129. M.I. acknowledges additional support from DFG Mercator Fellowship SPP1980. C.D.P. is supported by the U.S. DOE Office of Science, Office of Basic Energy Sciences, Division of Materials Sciences and Engineering, under contract DE-AC02-76SF00515 through NPNEQ at SLAC. Simulations were conducted at the U.S. DOE Office of Science, the National Energy Research Scientific Computing Center (NERSC), under contract DE-AC02-05CH11231. T.J.A.W., K.L., and A.A.C. acknowledge support by the AMOS program within the U.S. DOE Office of Science, Basic Energy Sciences (BES). J.P.F.N. was supported by the U.S. DOE Office of Science, Office of Basic Energy Sciences, under award DE-SC0014170. **Author contributions:** M.-F.L. and X.J.W. originated the project. A.A.C., T.J.A.W., X.J.W., and M.I. acquired funding. J.P.F.N., A.A.C., M.-F.L., K.L., J.Y., T.J.A.W., S.W., M.M., X.S., and X.J.W. designed and characterized the apparatus and executed experiments. M.K. provided laser support. M.-F.L., J.P.F.N., and K.L. analyzed experimental data. N.S., S.L., C.D.P., and M.I. provided theoretical calculations and interpretation of results. M.-F.L., N.S., S.L., M.M., T.J.A.W., A.A.C., C.D.P., and M.I. wrote the paper with comments from all authors. M.-F.L. coordinated the project. **Competing interests:** The authors declare no competing financial interests. **Data and materials availability:** The experimental data are available in the supplementary materials and Dryad (35).

SUPPLEMENTARY MATERIALS

science.org/doi/10.1126/science.abg3091
Materials and Methods
Supplementary Text
Figs. S1 to S7
References (36–48)

13 April 2021; accepted 6 July 2021
10.1126/science.abg3091

Imaging the short-lived hydroxyl-hydronium pair in ionized liquid water

M.-F. Lin^N, Singh^S, Liang^M, Mo^J, P. F. Nunes^K, Ledbetter^J, Yang^M, Kozina^S, Weathersby^X, Shen^A, A. Cordones^T, J. A. Wolf^C, D. Pemmaraju^M, Ihme^X, J. Wang

Science, 374 (6563), • DOI: 10.1126/science.abg3091

Capturing OH(HO) in ionized water

Recent advances in liquid-phase ultrafast electron diffraction techniques make it possible to observe what has only been theoretically presumed to occur at short times upon interaction of ionizing radiation with liquid water. Lin *et al.* provide direct evidence for capturing the short-lived radical-cation pair OH(HO), which has been hypothesized for years to form after ionization of liquid water but was not structurally resolved previously (see the Perspective by Cao *et al.*). The authors trace dissociation and subsequent nonradiative structural relaxation around the ionization center. —
YS

View the article online

<https://www.science.org/doi/10.1126/science.abg3091>

Permissions

<https://www.science.org/help/reprints-and-permissions>

Use of think article is subject to the [Terms of service](#)

Science (ISSN) is published by the American Association for the Advancement of Science, 1200 New York Avenue NW, Washington, DC 20005. The title *Science* is a registered trademark of AAAS.

Copyright © 2021 The Authors, some rights reserved; exclusive licensee American Association for the Advancement of Science. No claim to original U.S. Government Works